PROCEEDINGS OF SCIENCE

Dark matter in ATLAS and CMS

Bisnupriya Sahu[a,*] and **Bhawna Gomber**[a,b] on behalf of the ATLAS and CMS collaborations

[a] *School of Physics, University of Hyderabad, Prof C R Rao Road, Gachibowli, Hyderabad, Telangana, India*

[b] *CASEST, School of Physics , University of Hyderabad, Prof C R Rao Road, Gachibowli, Hyderabad, Telangana, India*

E-mail: bisnupriya.sahu@cern.ch, bhawna.gomber@cern.ch

The ATLAS and the Compact Muon Solenoid (CMS) used the proton-proton collision data with a center-of-mass energy of 13 TeV collected by the Large Hadron Collider (LHC) to carry out numerous searches for the existence of dark matter. This report mainly focuses on the Run II results of the independent dark matter searches using CMS and ATLAS detectors with the integrated luminosity of 139 fb^{-1}.

Corfu Summer Institute 2023 "School and Workshops on Elementary Particle Physics and Gravity" (CORFU2023)
23 April - 6 May , and 27 August - 1 October, 2023
Corfu, Greece

*Speaker

PoS(CORFU2023)088

1. Introduction

The existence of dark matter is known through astronomical observations, like the rotational curves of galaxies, bullet clusters, hot gas in clusters of galaxies, and cosmic microwave background (CMB) [1]. Since dark matter is electrically neutral and interacts only through gravity, it challenges the current detectors for their detection. One of the most powerful accelerators in today's world is the Large Hadron Collider (LHC), which comprises two beams, where the protons are accelerated in two opposite directions. These protons collide at four collision points, where four detectors are placed: ATLAS, CMS, LHCb, and ALICE. This report will briefly discuss the dark matter searches performed at ATLAS and CMS detectors.

2. Detectors

The ATLAS and CMS are two multipurpose detectors situated at the two collision points, point 1 and point 5, respectively, at LHC. ATLAS and CMS detectors' detailed information is available at [2] and [3], respectively.

3. Dark Matter Searches

The dark matter particles are massive, and their interactions with the visible matter are negligible, making it hard to detect them through the detectors. At LHC, the protons are collided, and dark matter is expected to be produced after the collision via the interaction of the SM particles. After the collision, the dark matter particles will fly away from both the CMS and ATLAS detector, which leads to the momentum imbalance in the transverse plane, known as the missing transverse momentum ($p_T{}^{miss}$). Therefore, the final state for these searches will seek a high momentum visible particle with large $p_T{}^{miss}$. Figure 1 shows the various dark matter searches performed at ATLAS and CMS. The following sections will briefly discuss the details of the searches performed at both experiments.

4. Mono-X searches

The mono-X search is the most common search for dark matter at ATLAS and CMS. In this search, there will be a high momentum SM particle (X) recoil against large $p_T{}^{miss}$, where X can be the jets, W or Z boson, photon, Higgs. This section will discuss the results of the mono-jet, mono-Z, and mono-Higgs analyses.

4.1 Mono-Jets

The experimental signature for mono-jet analysis is a high-momentum jet with a large amount of $p_T{}^{miss}$ in the final state. The Feynman diagram in Figure 2 shows the simplified model considered for this analysis where a jet is emitted as initial state radiation.

Both ATLAS [5] and CMS [6] performed a similar type of analysis with the Mono-jet search. In this analysis, the main physics object is to select a jet, which is reconstructed by a distance parameter of R = 0.4. Including this, CMS also looked up an additional jet, called the fatjets, with

Figure 1: Dark matter searches at ATLAS and CMS [4]

the R = 0.8. These fatjets include a deep neural network [7] to discriminate the jets originating from a vector boson's decay or QCD. The significant backgrounds in this analysis come from SM processes like Z($\to \nu\nu$) + jets and W($\to l\nu_l$) + jets, where a Z or the W boson is miss-reconstructed. Processes like single top, diboson, and multi jets also contributed to the background of this analysis. All these background processes are estimated through Monte Carlo simulations. To reduce the backgrounds in the analysis, the events with a single electron, muon, tau, or photon are vetoed. Also, a selection on the sizeable azimuthal angle, i.e. the $\Delta\phi$ in between the transverse momentum of the jet and the ${p_T}^{miss}$ is considered to reduce QCD multijet backgrounds.

A maximum bin likelihood fit is performed simultaneously on all the signal regions (SRs) and the controlled regions(CRs) to the ${p_T}^{miss}$ distribution. Figure 3 and Figure 4 shows the ${p_T}^{miss}$ distributions of ATLAS and CMS after the fitting, including the control regions. Figure 5a and Figure 5b show the exclusion region in the mediator mass and dark matter mass plane for the axial vector mediator observed at ATLAS [5] and CMS [6] respectively. At 95% CL, for low dark matter mass, ATLAS excludes the mediator mass up to 2.1 TeV, while CMS also excludes around 2.2 TeV.

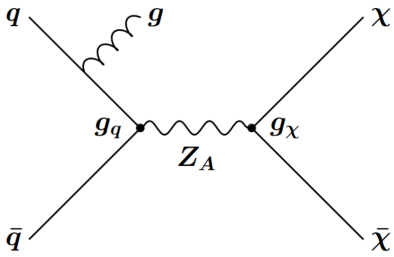

Figure 2: Feynman diagram of production of DM with axial-vector couplings exchanged with a mediator Z_A [5]

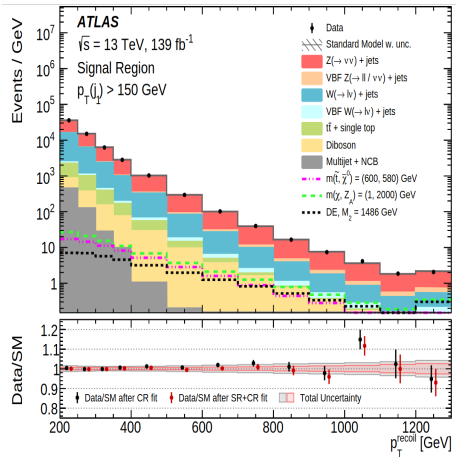

Figure 3: $p_T{}^{miss}$ distribution in signal region: ATLAS [5]

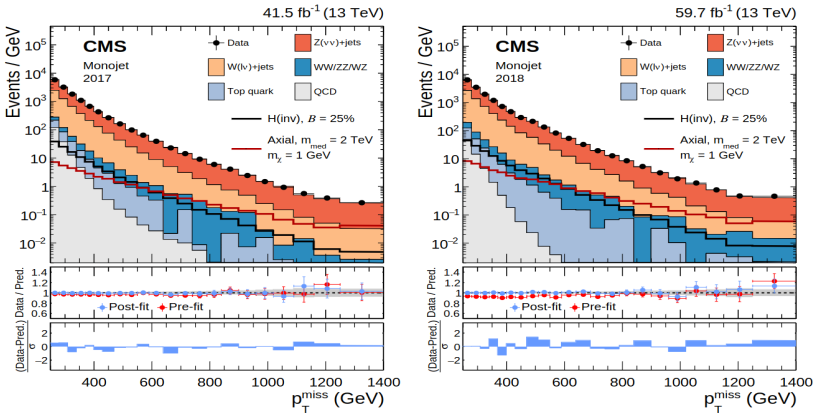

Figure 4: $p_T{}^{miss}$ distribution in signal region: 2017 (left) and 2018 (right) of CMS [6]

4.2 Mono-Z

The Mono-Z search looks for a Z boson, which further decays to two leptons and large $p_T{}^{miss}$ in the final state. Both ATLAS and CMS considered the 2HDM+a and simplified models in this analysis. Figure 6a and Figure 6b shows the Feynman diagram of these two models, respectively.

The major backgrounds for this analysis are the SM processes like ZZ ($Z \rightarrow \nu\nu$), WZ ($W \rightarrow l + \nu$), $t\bar{t}$, and WW. As the neutrinos leave no tracks in the detectors and if the lepton from

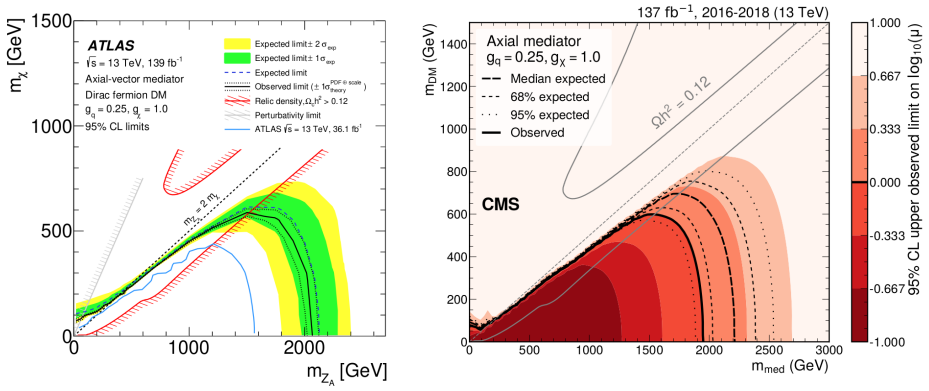

(a) ATLAS **(b)** CMS

Figure 5: At 95% CL, exclusion contour on the mediator mass and dark matter mass for axial vector mediator. (a) ATLAS [5], (b) CMS [6]

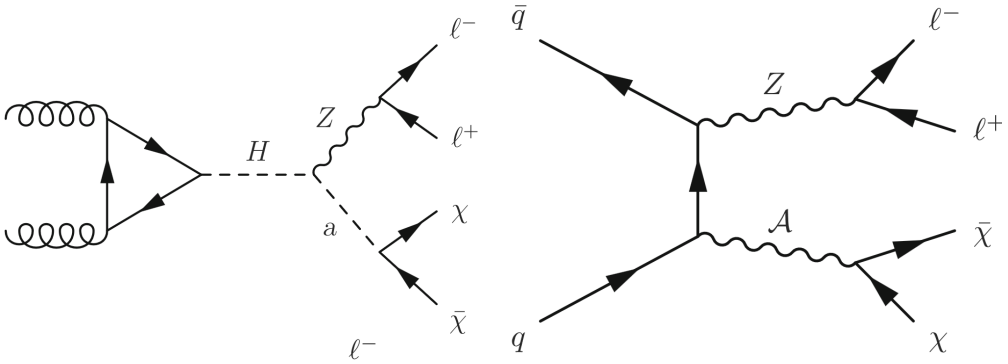

(a) **(b)**

Figure 6: Feynman diagram: (a) 2HDM+a model, (b) Simplified model (right) [9]

W boson falls outside the detector range, these two processes will mimic the signal final state. ATLAS [8] and CMS [9] considered three lepton & four lepton and eμ control regions (CRs) to constrain the backgrounds from ZZ & WZ and $t\bar{t}$& WW processes, respectively. The maximum likelihood fit is performed on the transverse mass M_T variable. Figure 7 shows the 2d scan of the two pseudo-scalar masses. At 95% CL upper limit set on the heavy pseudo-scalar mass, ATLAS as shown in Figure 7 (left), excludes the mediator mass up to 250-1700 GeV whereas, CMS shown in Figure 7 (right) excludes the mediator mass upto 250-1200 GeV, respectively.

4.3 Mono-Higgs

The discovery of Higgs opens up many possibilities in the search for physics beyond SM, where dark matter is one of them. Unlike the mono-jet and mono-Z searches, the Higgs boson production in ISR is highly suppressed. This analysis focuses on the decay of the Higgs boson to the SM particles like $b\bar{b}, \gamma\gamma, \tau\tau, W^+W^-$, or ZZ with significant $p_T{}^{miss}$. Both ATLAS [10] and CMS [12] considered the 2HDM+a model. The Feynman diagram of this model is shown in Figure 8. The major backgrounds and the event selection process for all the analyses fall under the monoHiggs

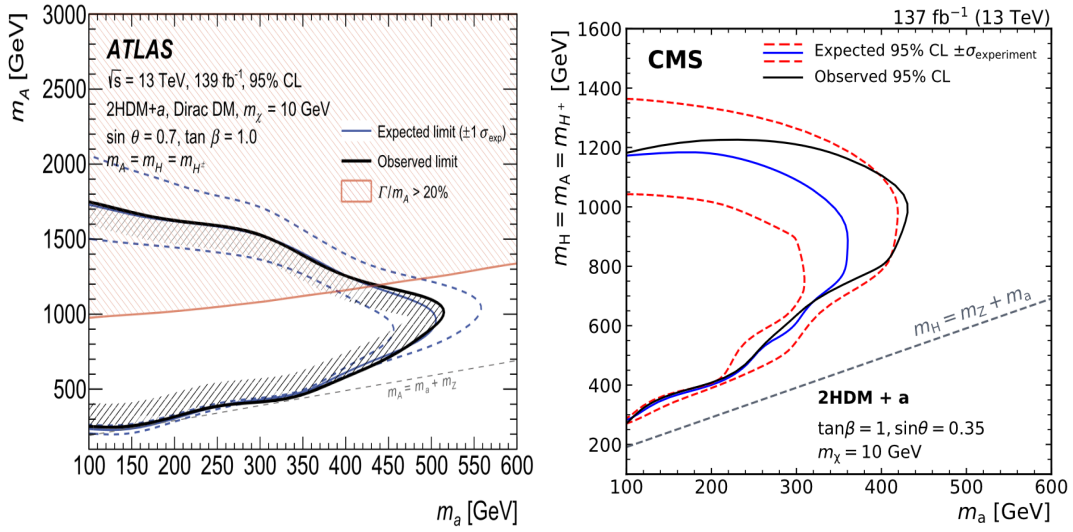

Figure 7: Exclusion region on the 2d scan of the two pseudo-scalar masses at 95% CL, Left: ATLAS [8], Right: CMS [9]

search are very similar. Like, In monoHiggs to taus analysis, where the Higgs boson decays to two tau leptons, the SM processes like VV, VH, $t\bar{t}$, V+jets, where V is the vector boson, are the major backgrounds. To reduce the multi-lepton backgrounds, this analysis considered vetoing the events if a third lepton is near the first two reconstructed leptons. On top of this selection, a jet veto is applied if it comes from the b-quark to reduce multijet backgrounds.

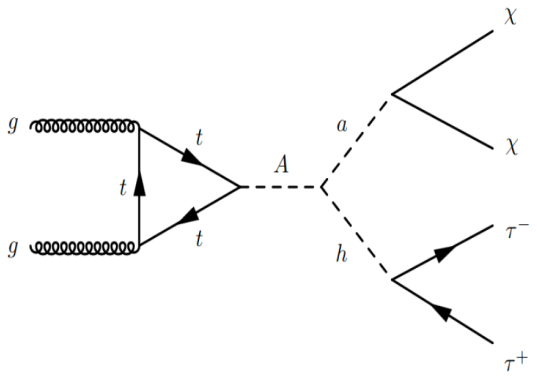

Figure 8: Feynman diagram of 2HDM+a model [10]

ATLAS performed a maximum likelihood fit on the sum of the transverse masses of the two leptons, i.e. $M_T{}^{\tau_1} + M_T{}^{\tau_2}$. Figure 9 (left) shows the full Run II results of ATLAS of the 2d scan of varying the pseudo-scalar masses A and a, and Figure 9 (right) shows the 2d scan of varying the heavy pseudo-scalar mass, and A and tanβ. At 95% CL, the upper limit on the heavy pseudo-scalar mass A is excluded up to 1000 GeV, for the other parameters of sinθ=0.35 and tanβ=1, and for low tanβ, the mass A is excluded up to 600 GeV at sinθ 0.7, and light pseudo-scalar, "a" at 250 GeV.

CMS also did a similar study in this analysis with 2HDM+a model, with 2016 data set, in the final state of Higgs decays to a pair of bottom quarks [12]. Figure 10 shows the 1d scan of the heavy

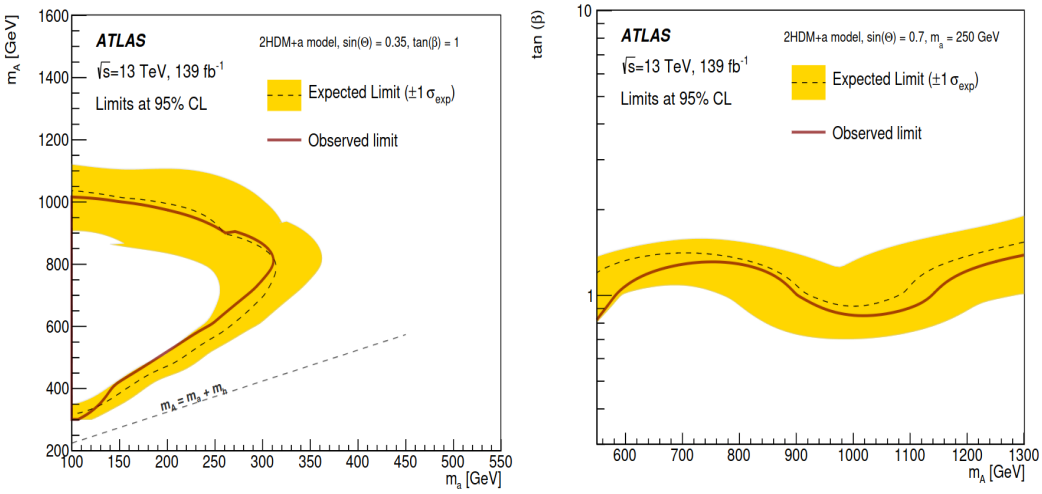

Figure 9: Left: Upper limit on the mediator mass A, m_A , Right: Upper limit on the tanβ, at 95% CL at ATLAS [10]

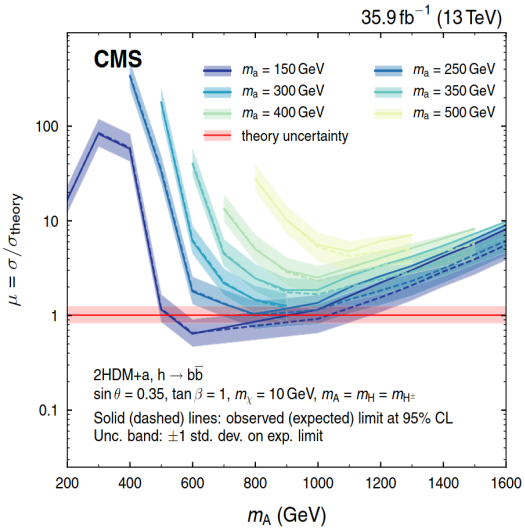

Figure 10: AT 95% CL upper limit on m_A for 2HDM+a model at CMS [12]

pseudo-scalar mass A, m_A. At 95% CL, the upper limit on m_A, CMS excludes m_A between 400-800 GeV, for sinθ=0.35 and tanβ=1. Along with this, CMS also studied this analysis in the combination of Higgs decays to $\rightarrow b\bar{b}, \gamma\gamma, \tau\tau, W^+W^-$, and ZZ with 2016 CMS data [11], with Z′-2HDM and Z′ baryonic model. Figure 11 (left) show the 2d scan varying the Z′ mass, $m_{Z'}$ and the dark matter m_χ with the Z′-2HDM and Figure 11 (right) shows for the Z′ baryonic model model,respectively. In the Z′-2HDM model, at 95% CL, the $m_{Z'}$ is excluded up to 500-3500 GeV, whereas in the Z′ baryonic model, it is excluded up to 2000 GeV.

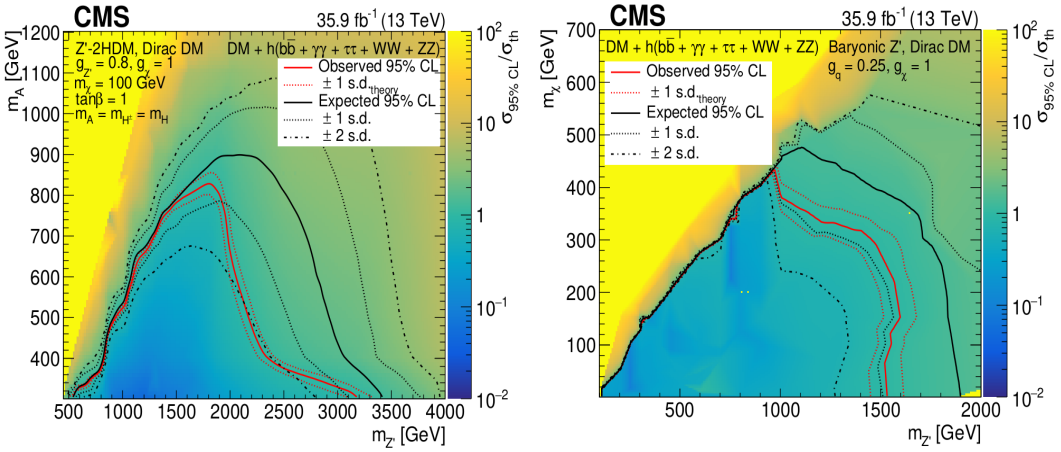

Figure 11: AT 95% CL the exclusion region in ($m_{Z'}$,m_{χ}) plane, Left: Z′-2HDM model, Right: Z′ baryonic model [11]

5. Higgs to invisible searches

This section will discuss the dark matter search in the invisible decay of the Higgs boson. It is believed that dark matter may interact with the Higgs boson as in the Higgs-portal model [13]. According to SM, the branching fraction of Higgs → invisible is only 0.1%, where the Higgs → ZZ^* → 4νs. If the Higgs boson decays to dark matter, the branching fraction will increase compared to SM. To investigate this, ATLAS [14] and CMS [15] considered the Vector Boson Fusion (VBF) production mode of Higgs → invisible. Figure 12 shows the Feynman diagram of VBF production of Higgs boson. The experimental signature for this analysis is the jets with large $p_T{}^{miss}$ coming from the Higgs boson decays invisibly.

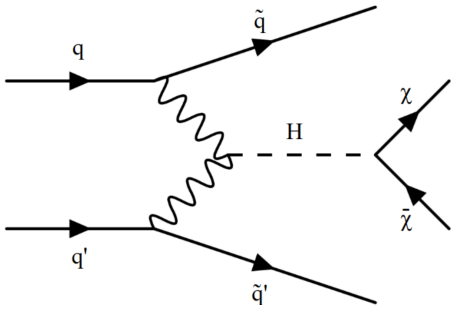

Figure 12: Feynman diagram of VBF production of Higgs → invisible [16]

ATLAS [14] and CMS [15] considered a similar type of event selection to select the events for this analysis. This analysis considered the events where two jets are of opposite charge and are well separated from each other with the condition $|\eta_{jj}| > 1$ to reduce multi-jet backgrounds. Also, a selection on $\Delta\phi$(two jets)<2.0 is applied to avoid the double counting of the leading jets. Adding to the above selections, the events with charged leptons and photons are also vetoed. The SM processes like Z(→ $\nu\nu$)+jets, W(→ $l+\nu$)+jets are the major background for this search, contributing a similar final state. These backgrounds are estimated through the lepton controlled regions (CRs).

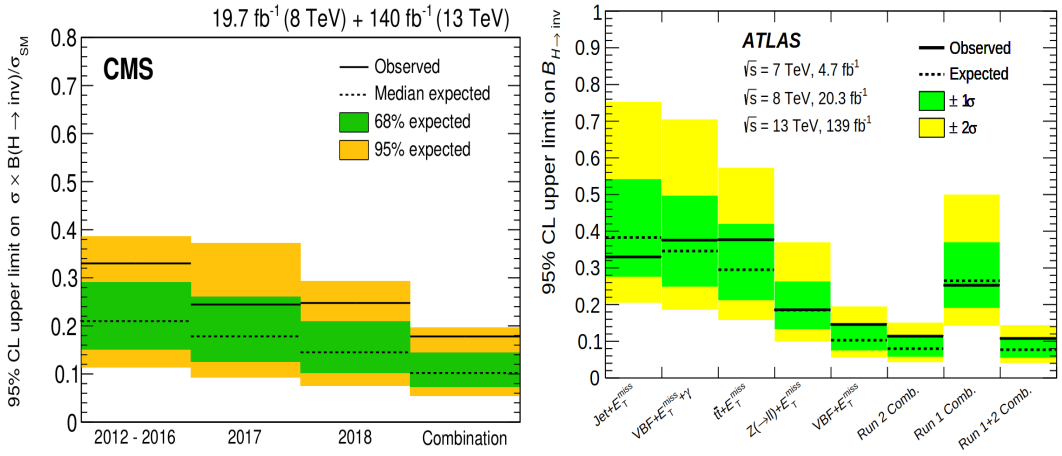

Figure 13: Combination results of the upper limits on the B(Higgs → invisible) at 95% CL, Left: CMS [15], Right: ATLAS [16]

A simultaneous maximum likelihood fit is performed on the mass distribution of two jets, m_{jj}. The upper limit is set on the branching fraction of H → invisible ($B(H \to inv)$) by considering the Higgs SM cross-sections. The CMS [15] reports the observed(expected) $B(H \to inv) < 0.18\ (0.10)$, shown in Figure 13 (left). Along with this, ATLAS performed a combination study in this analysis by considering different Higgs boson production modes like VBF + ${p_T}^{miss}$, Z → ll, $t\bar{t}$ + ${p_T}^{miss}$, jet + ${p_T}^{miss}$, (VBF + ${p_T}^{miss}$ + γ) [16]. ATLAS observed the $B(H \to inv) < 0.15(0.10)$ at 95% CL, shown in Figure 13 on the right.

6. Dark Higgs

Unlike the simplified DM models discussed in previous sections, the dark Higgs model explains how the mass of the particles in the dark sector is acquired. In this anlysis, CMS [17] looked for the dark Higgs (s), which decays into W^+W^- in the two leptons final state. Including the dark Higgs model, ATLAS [19] considered another model named the light vector model, where the Z′ will couple to the dark sector particles χ_1 and χ_2, and the heavy dark sector particle further decays to lighter dark matter particles in association with Z′ which decays leptonically. The Feynman diagrams of the dark Higgs model is shown in Figure 14 (left) and for light vector model is shown in Figure 14 (right). For the dark Higgs model, ATLAS considered the hadronic decay of the dark Higgs [18], whereas CMS considered the leptonic decay.

In this analysis both ATLAS and CMS considered the leptons with jets and large ${p_T}^{miss}$ in the final state. The SM processes like W ($\to l\nu$) + Jets, $t\bar{t}$, WW, Z ($\to \nu\nu$) are the major backgrounds for this analysis. The selected leptons for this analysis should be of opposite charge and different flavors to reduce the multilepton backgrounds. Along with this lepton selection, an event veto is also considered if a jet is tagged as a b-jet to reduce the multijet backgrounds.

A binned maximum likelihood is performed on the 2d distribution of dilepton mass, m_{ll} and the transverse mass in between the lepton and ${p_T}^{miss}$, ${m_T}^{l_{min}, {p_T}^{miss}}$. No significant excess is observed over the SM prediction, so the upper limit is set on the production of the dark matter in the dark Higgs model. Figure 15 shows the observed(expected) exclusion region reported by CMS in the

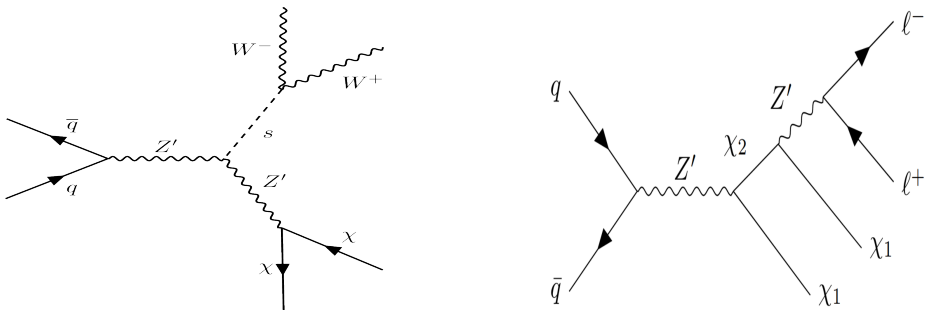

Figure 14: Left: Feynman diagram of Dark Higgs model [17], Right: Feynman diagram of light-vector model [19]

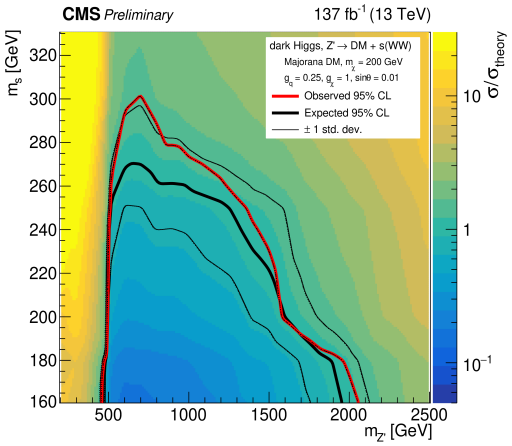

Figure 15: CMS [17] observed (expected) exclusion regions for the dark Higgs model in the (m_s, $m_{Z'}$) plane at 95% CL

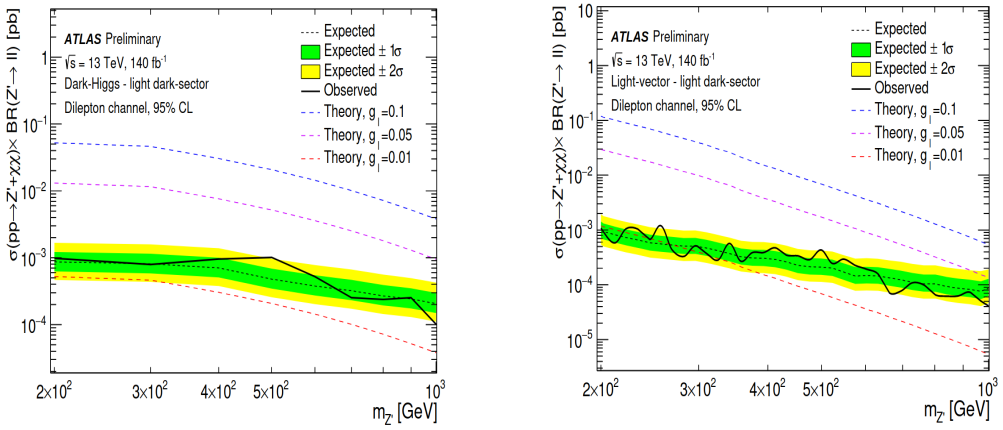

Figure 16: ATLAS [19] limits on the crosssection for light dark-sector, Left: for dark Higgs model, Right: light vector model, in the dilepton channel, at 95% CL

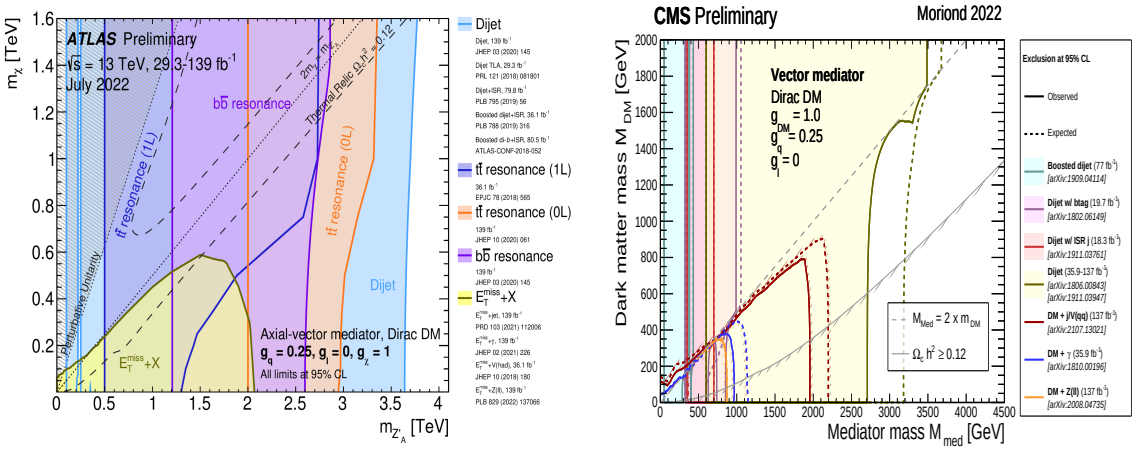

Figure 17: Dark summary plots with a vector mediator in simplified model. Left: ATLAS [21], Right: CMS [20]

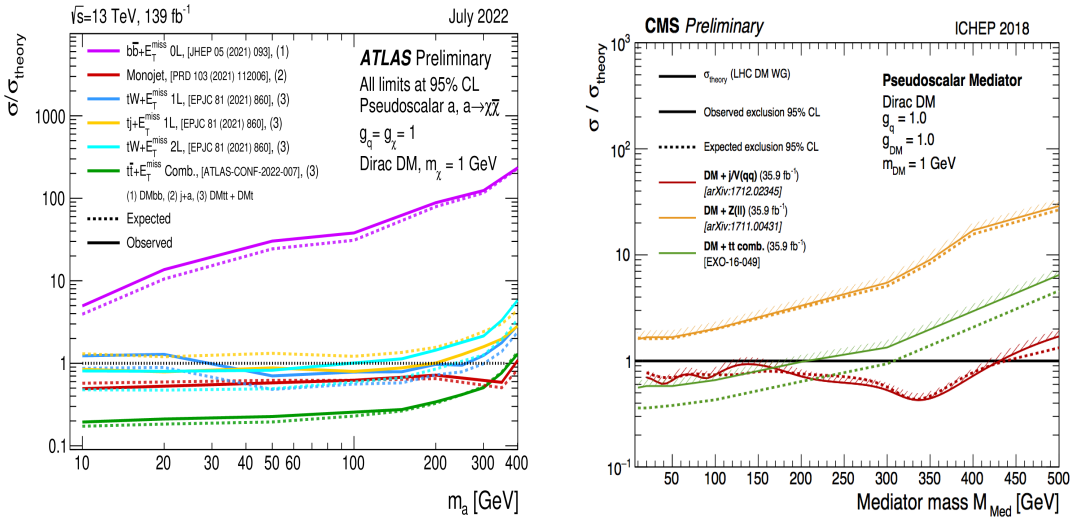

Figure 18: Dark summary plots with a pseudoscalar mediator in simplified model. Left: ATLAS [21], Right: CMS [20]

m_s and m'_Z. The observed (expected) limits of ATLAS experiment [19] on the cross-section for the light-dark sector in the Dilepton channel, with dark Higgs model as shown in Figure 16 (left) and light vector model as shown in Figure 16 (right), respectively. At 95% CL, for the dark Higgs model, CMS [17] excludes the Z' mass in between 500-2000 GeV, whereas ATLAS sets the limits on the cross-section for the light-dark sector: $1.5 \cdot 10^{-3}$ to $3 \cdot 10^{-4} pb$ and $1 \cdot 10^{-3}$ to $3 \cdot 10^{-5} pb$ for the dark Higgs model and light vector model, respectively, shown in Figure 16.

7. Dark matter Summary plots from ATLAS and CMS

Both the experiments, ATLAS and CMS, perform various dark matter searches and provide summary plots after the combinations of all the searches based on the models.

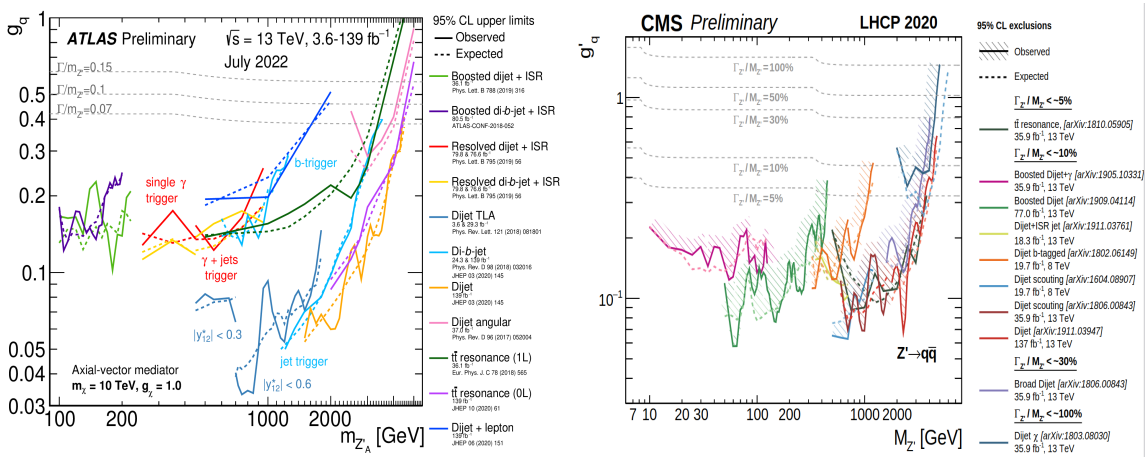

Figure 19: Dark summary plots of the coupling constants in simplified model. Left: ATLAS [21], Right: CMS [20]

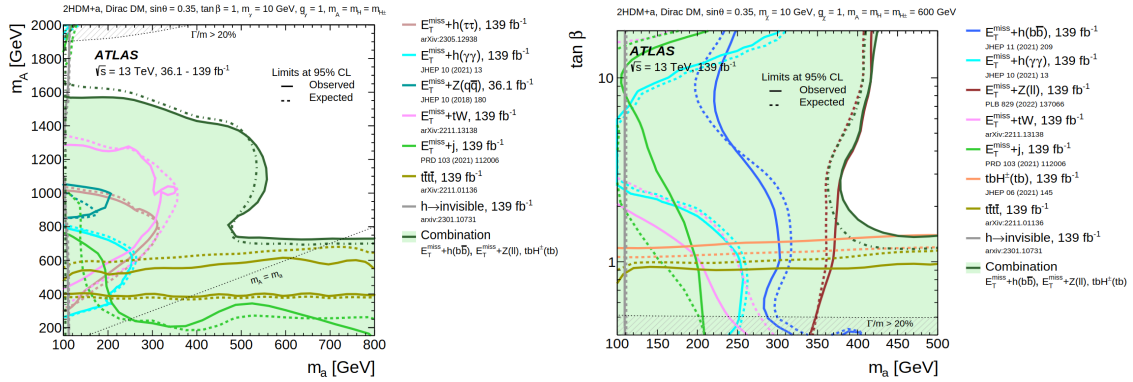

Figure 20: ATLAS [22], Left: Observed (expected) exclusion regions at 95% CL in the 2HDM+a model, in (m_a, m_A) plane, Right: Observed (expected) exclusion regions at 95% CL in the 2HDM+a model, in (m_a, tanβ) plane

The exclusion region of the mass of the vector mediator ($M_{mediator}$) vs the mass of the dark matter (M_{DM}), at 95% CL with the coupling constant, $g_q = 0.25$, $g_\chi = 1$, of ATLAS [21] is shown in Figure 17 (left) and for CMS [20] is shown in Figure 17 (right), respectively. In addition to this, the exclusion region of $M_{mediator}$, where the mediator is a pseudoscalar at coupling constant, $g_q = g_\chi = 1$, of ATLAS [21] is shown in Figure 18 (left) and of CMS [20] is shown in Figure 18 (right), respectively. Similarly, the exclusion limit on the coupling (g_q, $M_{mediator}$) plane for the simplified model of ATLAS [21] is shown in Figure 19 (left) and of CMS [20] is shown in Figure 19 (right), respectively. The observed (expected) exclusion limits for various analyses are represented by the solid (dashed) lines for both experiments.

In addition to the summary plots, ATLAS [22] also combined many dark matter searches for the 2HDM+a model. The observed (expected) limits on the plane of pseudoscalar masses is shown in Figure 20 (left) and in the ($m_A, tan\beta$) plane is shown in Figure 20 (right) after combining all the searches with this model.

8. Summary

The ATLAS and CMS experiments have brought up numerous searches for the mysterious dark matter, exploring a wide range of final states. This report summarized a few of them. Although all these analyses observed no dark matter signal. The improvements in the analysis techniques and tools, with good background modeling and estimation with new signal models for the searches in the near future with the upcoming data, will continue its quest for the dark matter at LHC.

References

[1] N. Aghanim, Y. Akrami, F. Arroja, M. Ashdown, J. Aumont, C. Baccigalupi, M. Ballardini, A. J. Banday, et al. *Planck 2018 results*, Astronomy Astrophysics, 641:A1, Sep 2020, doi: 10.10510004-6361/201833880, https://doi.org/10.1051/0004-6361/201833880

[2] The ATLAS Collaboration., *The ATLAS Experiment at the CERN Large Hadron Collider*, Journal of Instrumentation, 3(08):S08003, Aug 2008, doi: 10.1088/1748-0221/3/08/S08003, https://dx.doi.org/10.1088/1748-0221/3/08/S08003

[3] The CMS Collaboration., *The CMS experiment at the CERN LHC*, Journal of Instrumentation, 3(08):S08004, Aug 2008, doi: 10.1088/1748-0221/3/08/S08004, https://dx.doi.org/10.1088/1748-0221/3/08/S08004.

[4] Danyer Perez Adan, *Dark Matter searches at CMS and ATLAS*, arXiv:2301.10141, doi:10.48550/arXiv.2301.10141, https://doi.org/10.48550/arXiv.2301.10141

[5] ATLAS Collaboration., *Search for new phenomena in events with an energetic jet and missing transverse momentum* Phys. Rev. D, 103(11):112006, 2021. https://arxiv.org/abs/2102.10874

[6] CMS Collaboration., *Search for new particles in events with energetic jets and large missing transverse momentum*, JHEP, 11:153, 2021. https://link.springer.com/article/10.1007/JHEP11(2021)153

[7] CMS Collaboration., *Identification of heavy, energetic, hadronically decaying particles using machine-learning techniques*, Journal of Instrumentation, doi:10.1088/1748-0221/15/06/P06005, https://dx.doi.org/10.1088/1748-0221/15/06/P06005

[8] ATLAS collaboration., *Search for associated production of a Z boson with an invisibly decaying Higgs boson or dark matter candidates at s=13 TeV with the ATLAS detector*, Physics Letters B, https://www.sciencedirect.com/science/article/pii/S0370269322002003

[9] CMS Collaboration., *Search for dark matter produced in association with a leptonically decaying boson in proton–proton collisions*, Eur. Phys. J. C 81, 13 (2021). https://doi.org/10.1140/epjc/s10052-020-08739-5

[10] ATLAS collaboration., *Search for dark matter produced in association with a Higgs boson decaying to tau leptons at $\sqrt{s} = 13$ TeV with the ATLAS detector*, J. High Energ. Phys. 2023, http://dx.doi.org/10.1007/JHEP09(2023)189

[11] CMS Collaboration., *Search for dark matter particles produced in association with a Higgs boson in proton-proton collisions at $\sqrt{s} = 13$ TeV* , J. High Energ. Phys. 2020, 25 (2020), https://doi.org/10.1007/JHEP03(2020)025

[12] CMS Collaboration., *Search for dark matter produced in association with a Higgs boson decaying to a pair of bottom quarks in proton–proton collisions at $\sqrt{s} = 13$ TeV* , Eur. Phys. J. C 79, 280 (2019). https://doi.org/10.1140/epjc/s10052-019-6730-7

[13] Arcadi, Giorgio and Djouadi, Abdelhak and Raidal, Martti et al. *Dark Matter through the Higgs portal*, Physics Reports (2020), doi: 10.1016/j.physrep.2019.11.003, http://dx.doi.org/10.1016/j.physrep.2019.11.003

[14] ATLAS collaboration., *Search for invisible Higgs-boson decays in events with vector-boson fusion signatures using 139 fb^{-1} of proton-proton data recorded by the ATLAS experiment*, Journal of High Energy Physics (2022), doi: 10.1007/jhep08(2022)104, http://dx.doi.org/10.1007/JHEP08(2022)104,

[15] CMS Collaboration., *Search for invisible decays of the Higgs boson produced via vector boson fusion in proton-proton collisions at* $\sqrt{s}$ = 13 TeV, Phys. Rev. D (2022), doi: 10.1103/PhysRevD.105.092007, https://link.aps.org/doi/10.1103/PhysRevD.105.092007

[16] ATLAS collaboration., *Combination of searches for invisible decays of the Higgs boson using 139 fb^{-1} of proton-proton collision data at* $\sqrt{s}$ = 13 TeV *collected with the ATLAS experiment*, Phys. Lett. B 842 (2023) 137963, doi: 10.1016/j.physletb.2023.137963, https://www.sciencedirect.com/science/article/pii/S0370269323002976

[17] CMS Collaboration., *Search for dark matter particles produced in association with a dark Higgs boson decaying into W^+W^- in proton-proton collisions at* $\sqrt{s}$ = 13 TeV *with the CMS detector*, https://cds.cern.ch/record/2776774/files/EXO-20-013-pas.pdf

[18] ATLAS collaboration., *Search for Dark Matter Produced in Association with a Dark Higgs Boson Decaying into $W^{\pm}W^{\mp}$ or ZZ in Fully Hadronic Final States from* $\sqrt{s}$ = 13 TeV *pp Collisions Recorded with the ATLAS Detector*, PhysRevLett.126.121802,https://link.aps.org/doi/10.1103/PhysRevLett.126.121802

[19] ATLAS collaboration., *Search for a new leptonically decaying neutral vector boson in association with missing transverse energy in proton–proton collisions at* $\sqrt{s}$ = 13 TeV *with the ATLAS detector*, https://atlas.web.cern.ch/Atlas/GROUPS/PHYSICS/CONFNOTES/ATLAS-CONF-2023-045/ATLAS-CONF-2023-045.pdf

[20] CMS-EXOTICA-Summary, https://twiki.cern.ch/twiki/bin/view/CMSPublic/SummaryPlotsEXO13TeV [Accessed 22-03-2024]

[21] ATL-PHYS-PUB-2023-018, https://atlas.web.cern.ch/Atlas/GROUPS/PHYSICS/PUBNOTES/ATL-PHYS-PUB-2023-018/ [Accessed 22-03-2024]

[22] ATLAS collaboration., *Combination and summary of ATLAS dark matter searches interpreted in a 2HDM with a pseudo-scalar mediator using 139 fb^{-1} of $\sqrt{s}$ = 13 TeV pp collision data*, https://doi.org/10.48550/arXiv.2306.00641